

the opposite wall of the male's home enclosure. Investigation and scent marking were measured as described above. Tests were conducted four days apart in balanced order. Before tests, a female was introduced into each male's enclosure for 24 h, the female was then removed and males in neighbour enclosures were allowed a single interaction to stimulate more males to show competitive scent marking. Eleven out of 15 subjects deposited at least 20 marks on each tile and were included in analysis.

Received 16 August; accepted 17 September 2001.

1. Brown, R. E. & McDonald, D. W. *Social Odours in Mammals* Vols 1 & 2 (Clarendon, Oxford, 1985).
2. Yamazaki, K., Singer, A. & Beauchamp, G. K. Origin, functions and chemistry of H-2 regulated odorants. *Genetica* **104**, 235–240 (1999).
3. Yamazaki, K. *et al.* Sensory distinction between H-2b and H-2bm1 mutant mice. *Proc. Natl Acad. Sci. USA* **80**, 5685–5688 (1983).
4. Singh, P. B., Brown, R. E. & Roser, B. MHC antigens in urine as olfactory recognition cues. *Nature* **327**, 161–146 (1987).
5. Beynon, R. J., Robertson, D. H. L., Hubbard, S. J., Gaskell, S. J. & Hurst, J. L. in *Advances in Chemical Communication in Vertebrates* (eds Johnston, R. E., Muller-Schwarze, D. & Sorensen, P.) 137–147 (Plenum, New York, 1999).
6. Bacchini, A., Gaetani, E. & Cavagioni, A. Pheromone binding proteins of the mouse, *Mus musculus*. *Experientia* **48**, 419–421 (1992).
7. Robertson, D. H. L., Beynon, R. J. & Evershed, R. P. Extraction, characterization and binding analysis of two pheromonally active ligands associated with major urinary protein of house mouse (*Mus musculus*). *J. Chem. Ecol.* **19**, 1405–1416 (1993).
8. Beynon, R. J. *et al.* in *Chemical Signals in Vertebrates* (eds Marchelewska-Koj, A., Muller-Schwarze, D. & Lepri, J.) 149–156 (Plenum, New York, 2001).
9. Hurst, J. L., Robertson, D. H. L., Tolladay, U. & Beynon, R. J. Proteins in urine scent marks of male house mice extend the longevity of olfactory signals. *Anim. Behav.* **55**, 1289–1297 (1998).
10. Humphries, R. E., Robertson, D. H. L., Beynon, R. J. & Hurst, J. L. Unravelling the chemical basis of competitive scent marking in house mice. *Anim. Behav.* **58**, 1177–1190 (1999).
11. Mucignat-Caretta, C. & Caretta, A. Urinary chemical cues affect light avoidance behaviour in male laboratory mice, *Mus musculus*. *Anim. Behav.* **57**, 765–769 (1999).
12. Jemiolo, D., Alberts, J., Sochinski-Wiggins, S., Harvey, S. & Novotny, M. Behavioural and endocrine responses of female mice to synthetic analogs of volatile compounds in male urine. *Anim. Behav.* **33**, 1114–1118 (1985).
13. Novotny, M. V., Ma, W., Wiesler, D. & Zidek, L. Positive identification of the puberty-accelerating pheromone of the house mouse: the volatile ligands associating with the major urinary protein. *Proc. R. Soc. Lond. B* **266**, 2017–2022 (1999).
14. Jemiolo, B., Harvey, S. & Novotny, M. Promotion of the Whitten effect in female mice by synthetic analogs of male urinary constituents. *Proc. Natl Acad. Sci. USA* **83**, 4576–4579 (1986).
15. Marchelewska-Koj, A., Cavagioni, A., Mucignat-Caretta, C. & Olejniczak, P. Stimulation of estrus in female mice by male urinary proteins. *J. Chem. Ecol.* **26**, 2355–2366 (2000).
16. Novotny, M., Harvey, S., Jemiolo, B. & Alberts, J. Synthetic pheromones that promote inter-male aggression in mice. *Proc. Natl Acad. Sci. USA* **82**, 2059–2061 (1985).
17. Brennan, P. A., Schellinck, H. M. & Keverne, E. B. Patterns of expression of the immediate-early gene *egr-1* in the accessory olfactory bulb of female mice exposed to pheromonal constituents of male urine. *Neuroscience* **90**, 1463–1470 (1999).
18. Nevison, C. M., Barnard, C. J., Beynon, R. J. & Hurst, J. L. The consequences of inbreeding for recognising competitors. *Proc. R. Soc. Lond. B* **267**, 687–694 (2000).
19. Hurst, J. L. *et al.* in *Chemical Signals in Vertebrates* (eds Marchelewska-Koj, A., Muller-Schwarze, D. & Lepri, J.) 43–50 (Plenum, New York, 2001).
20. Bishop, J. O., Clark, A. J., Clissold, P. M., Hainey, S. & Francke, U. Two main groups of mouse major urinary protein genes, both largely located on chromosome 4. *EMBO J.* **1**, 615–620 (1982).
21. Robertson, D. H., Cox, K. A., Gaskell, S. J., Evershed, R. P. & Beynon, R. J. Molecular heterogeneity in the major urinary proteins of the house mouse *Mus musculus*. *Biochem. J.* **316**, 265–272 (1996).
22. Payne, C. E. *et al.* in *Chemical Signals in Vertebrates* (eds Marchelewska-Koj, A., Muller-Schwarze, D. & Lepri, J.) 233–240 (Plenum, New York, 2001).
23. Hurst, J. L. Urine marking in populations of wild house mice *Mus domesticus* Ruttly. 1. Communication between males. *Anim. Behav.* **40**, 209–222 (1990).
24. Lücke, C. *et al.* Solution structure of a recombinant mouse major urinary protein. *Eur. J. Biochem.* **266**, 1210–1218 (1999).
25. Novotny, M., Harvey, S. & Jemiolo, B. Chemistry of male dominance in the house mouse, *Mus domesticus*. *Experientia* **46**, 109–113 (1990).
26. Krieger, J. *et al.* Selective activation of G protein subtypes in the vomeronasal organ upon stimulation with urine-derived compounds. *J. Biol. Chem.* **274**, 4655–4662 (1999).
27. Marie, A. D. *et al.* Effect of polymorphisms on ligand binding by mouse major urinary proteins. *Protein Sci.* **10**, 411–417 (2001).
28. Singer, A. G., Tsuchiya, H., Wellington, J. L., Beauchamp, G. K. & Yamazaki, K. Chemistry of odortypes in mice—fractionation and bioassay. *J. Chem. Ecol.* **19**, 569–579 (1993).
29. Singer, A. G., Beauchamp, G. K. & Yamazaki, K. Volatile signals of the major histocompatibility complex in male mouse urine. *Proc. Natl Acad. Sci. USA* **94**, 2210–2214 (1997).
30. Pearce-Pratt, R., Schellinck, H., Brown, R., Singh, P. B. & Roser, B. Soluble MHC antigens and olfactory recognition of genetic individuality: the mechanism. *Genetica* **104**, 223–230 (1999).

## Acknowledgements

This work was supported by Biotechnology and Biological Sciences Research Council (BBSRC) grants to J.L.H. and R.J.B., a BBSRC studentship to C.E.P. and an Egyptian government scholarship to A.D.M.

## Competing interests statement

The authors declare that they have no competing financial interests.

Correspondence and requests for materials should be addressed to J.L.H. (e-mail: jane.hurst@liverpool.ac.uk).

# Drosophila Stardust interacts with Crumbs to control polarity of epithelia but not neuroblasts

Yang Hong<sup>\*</sup>, Beth Stronach<sup>†</sup>, Norbert Perrimon<sup>†</sup>, Lily Yeh Jan<sup>\*</sup> & Yuh Nung Jan<sup>\*</sup>

<sup>\*</sup> Howard Hughes Medical Institute, Department of Physiology and Biochemistry, University of California San Francisco, San Francisco, California 94143-0725, USA

<sup>†</sup> Department of Genetics, Harvard Medical School, 200 Longwood Avenue, Boston, Massachusetts 02115, USA

Establishing cellular polarity is critical for tissue organization and function. Initially discovered in the landmark genetic screen for *Drosophila* developmental mutants<sup>1–4</sup>, *bazooka*, *crumbs*, *shotgun* and *stardust* mutants exhibit severe disruption in apicobasal polarity in embryonic epithelia, resulting in multilayered epithelia, tissue disintegration, and defects in cuticle formation<sup>5</sup>. Here we report that *stardust* encodes single PDZ domain MAGUK (membrane-associated guanylate kinase) proteins that are expressed in all primary embryonic epithelia from the onset of gastrulation. *Stardust* colocalizes with *Crumbs*<sup>6</sup> at the apicolateral boundary, although their expression patterns in sensory organs differ. *Stardust* binds to the carboxy terminus of *Crumbs* *in vitro*, and *Stardust* and *Crumbs* are mutually dependent in their stability, localization and function in controlling the apicobasal polarity of epithelial cells. However, for the subset of ectodermal cells that delaminate and form neuroblasts, their polarity requires the function of *Bazooka*<sup>7,8</sup>, but not of *Stardust* or *Crumbs*.

The *stardust* (*sdt*) mutation is not complemented by *Df(1)HA11*, a deletion of regions 7D14–7D22 (ref. 9). *HA11* was mapped to a region of about 85 kilobases (kb) (B.S., unpublished data), predicted to contain six open reading frames of more than 300 amino acids each by the genome annotation database of *Drosophila* (GadFly, <http://www.bdgp.org>). One of these open reading frames, CG1617, encodes a previously unknown MAGUK protein containing a single PDZ (PSD-95, Discs Large, ZO-1) domain, a SH3 (Src homology region 3) domain and a GUK (guanylate kinase) domain. We pursued the possibility that this MAGUK protein corresponds to *Sdt*, because other proteins with similar motifs are important for cell–cell junctions and cellular polarity<sup>10–14</sup>.

To obtain full-length complementary DNAs, we screened an embryonic cDNA library and identified a large transcription unit that includes CG1617 and CG15341. Three cDNAs for this *sdt* candidate gene, *sdt1*, *sdt2* and *sdt3* (Fig. 1a), differ at their 5' ends owing to alternative splicing, and code for two isoforms of potential *Sdt* protein: *SdtA*, with 1,292 amino acids; and *SdtB*, with 860 amino acids and lacking the 432 amino acids encoded by alternatively spliced exon 3 (hatched bar in Fig. 1d). *In vitro* translation of *sdt1* and *sdt3* yielded products of the predicted size (Fig. 1b). Blast analyses (<http://www.ncbi.nlm.nih.gov/BLAST>) identified homologues of *SdtB* in mouse, recently identified as Pals1 (proteins associated with mammalian Lin-7 (ref. 15), and in *Caenorhabditis elegans* a predicted protein of unknown function (see Supplementary Information). No homology to the amino-acid sequence of exon 3 in *SdtA* was found.

The gene that gives rise to these three cDNAs is *sdt*, because three independent strong hypomorphic or null alleles of *sdt*—*XN05*, *XP96* and *EH*—induced by ethylmethane sulphonate (EMS)<sup>9,16</sup> each carry a single nucleotide alteration in the coding sequences for *sdt1*–3. *XN05* contains a nonsense mutation in exon 6 (Fig. 1d). *XP96* contains a mutation at the 3' splice junction of exon 6; a failed splicing would incorporate a stop codon that immediately follows

this splice junction. *EH* contains a nonsense mutation in exon 3, which should eliminate SdtA but not SdtB, indicating that SdtA serves a critical function in embryogenesis.

Affinity-purified rabbit antibodies against a glutathione S-transferase (GST) fusion of the C-terminal 200 amino acids common to

SdtA and SdtB clearly outlined epithelial cells in wild-type embryos (Fig. 1c, right), but not in zygotic *XN05* (Fig. 1c, left) or *XP96* mutant embryos (data not shown). The speckles seen in mutant as well as wild-type embryos are background nonspecific staining. From the onset of gastrulation (stage 5 or 6), Sdt is expressed

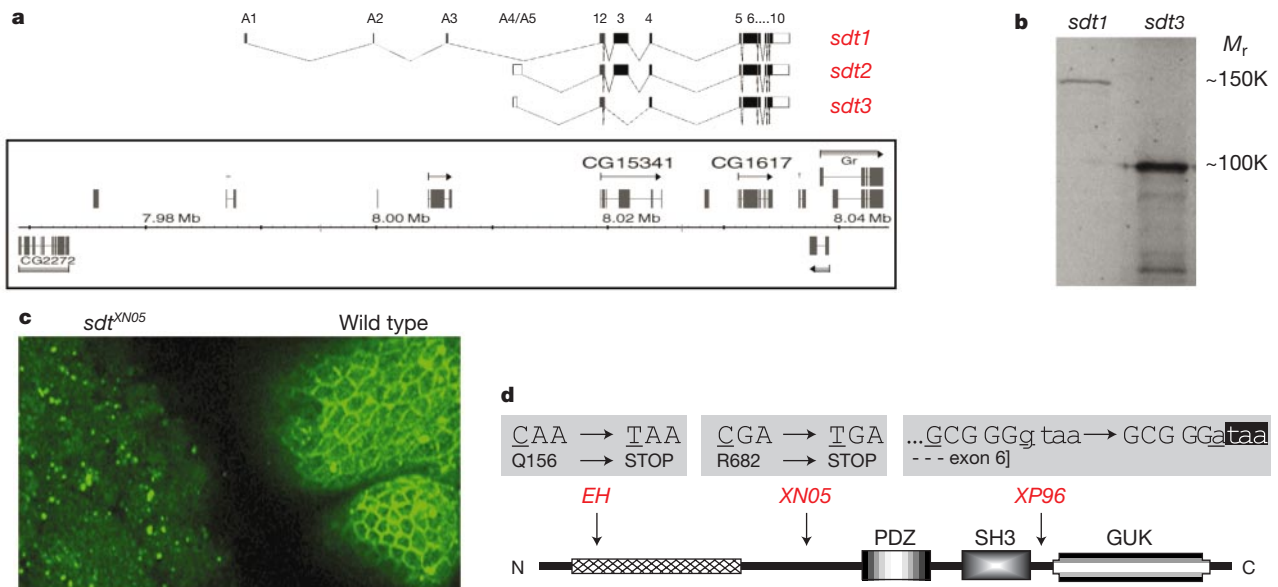


**Figure 1** Cloning of *sdt*. **a**, Three alternatively spliced cDNA isoforms of *sdt*. Upstream noncoding exons are designated as A1–A5, and the exon that includes the first in-frame ATG is designated as exon 1. Boxed is a modified GadFly screen display of the 7D18 region of the X chromosome, with arrows indicating the direction of transcription, and bars indicating predicted exons. **b**, *In vitro* translation products of *sdt1* and *sdt3* cDNAs. Each cDNA yields a major protein product of the expected size: relative molecular mass ( $M_r$ )

~150,000 (150K) for SdtA and ~100K for SdtB. **c**, Sdt antibody outlines epithelial cells in wild-type but not *sdt<sup>XN05</sup>* zygotic mutant embryo. Both embryos are at about stage 11. The speckles shown in the *XN05* embryo are nonspecific background staining. **d**, SdtA protein structure and lesions in three *sdt* alleles. Hatched bar represents the amino-acid sequence of the alternatively spliced exon 3.

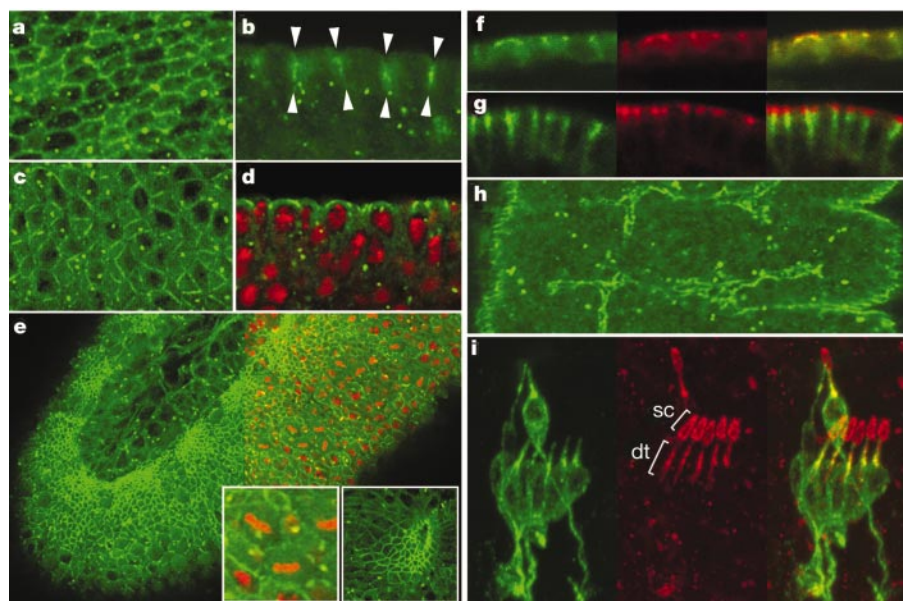


**Figure 2** Developmental expression pattern of Sdt. **a, b**, Sdt is first detectable around stage 5–6, and is enriched at the boundary between epithelial cells, seen in tangential section (**a**) and cross section (**b**) of embryos. Vertical pairs of arrowheads in **b** highlight the Sdt distribution along the apicolateral cortex. **c, d**, At stage 8–9 Sdt concentrates around apical cell boundaries as seen in tangential section (**c**) and cross section (**d**) of the same embryo, with DNA stained by propidium iodide (PI) (red) in **d**. **e**, A honeycomb pattern of Sdt forms at stage 9. The right half is superimposed with DNA staining (red). The left inset shows that in cells undergoing mitosis, Sdt staining is diffuse or absent from the cell boundary. The right inset shows that Sdt is further enriched at the sites of contraction of

the apical cell surface during cell invagination (a tracheal pit is shown here). **f, g**, Cross section of a stage 13 (**f**) and a stage 14 (**g**) embryo. Sdt (red) overlaps with AJ marker Arm (green, **f**) but extends further apically. Sdt is apical to the septate junction marker Cor (green, **g**) with no overlap. **h**, Sdt expression at the apical lumen surface of the developing tracheal system in a stage 13 embryo. Anterior is up and dorsal left. **i**, Chordotonal organs double stained with Sdt antibody (red) and 22C10 (green), which specifically stains neurons of the peripheral and central nervous systems. Sdt is localized to the dendritic tips (dt) and scolopales (sc). In **f, g** and **i**, right panels are merged images.

around the apical cell boundaries (Fig. 2a) and the apical region of the lateral cortex (Fig. 2b). In late gastrulation, coincident with formation of the zonula adherens (ZA), Sdt starts to form a solid continuous belt around the apical boundary of epithelial cells, and is also enriched at the apical surface (Fig. 2c–e). Sdt distribution overlaps with adherens junction markers Armadillo (Arm) and DE-cadherin (DE-cad), although Sdt seems to localize slightly apical to adherens junctions (Fig. 2f) as well. When septate junctions form at the basolateral side of epithelial cells (embryonic stage 13 or 14), Sdt retains its apical localization and association with the ZA, and does not overlap with the septate junction marker Coracle (Cor) (Fig. 2g). The tracheal system, foregut and hindgut, which are part of the primary epithelia<sup>17</sup>, also express Sdt at their apical surface (Fig. 2h). Apical lateral subcellular distribution of Sdt persists throughout embryonic development in epithelia, although the expression gradually decrease in stages 16 and 17. Sdt is also expressed in sensory organs. For example, in antennomaxillary complexes and chordotonal organs, strong Sdt staining is seen on the dendritic tips of sensory neurons and scolopale lumen formed by support scolopale cells (Fig. 2i).

Adherens junctions (AJs) first form during cellularization (stage 5) in fly embryos as spot AJs<sup>17,18</sup>, which later migrate apically and coalesce to form the ZA, a continuous belt-like AJ around the apical lateral cell boundary<sup>19</sup>. The *sdt* mutations seem to specifically disrupt the fusion of apically localized spot AJs to form the ZA<sup>19,20</sup>. In *sdt* zygotic mutants, AJ/ZA components Arm and DE-cad fail to form a smooth honeycomb pattern, but appear significantly fragmented<sup>16,19,20</sup> (see Fig. 3j, k; and data not shown). This failure of ZA formation and apicobasal polarity establishment results in an irregular and multilayered epithelial structure in later embryogenesis<sup>9</sup> (Fig. 3b). Despite their initial normal distribution during gastrulation (stage 7 or 8), basolateral localization of Discs Large (Dlg) and Scribble (Scrib), which marks the future septate junctions, is progressively compromised in later stages (Fig. 3b, e). Another indication that septate junctions fail to develop in *sdt* mutants was the cytoplasmic distribution of the septate junction

**Table 1** Localization of cellular polarity markers in stage 9–13 embryos

| Protein        | Localization in wild-type embryos |            | Localization in <i>sdt</i> embryos |            | Reduction of protein level in <i>sdt</i> mutant |
|----------------|-----------------------------------|------------|------------------------------------|------------|---|
|                | Epithelia                         | Neuroblast | Epithelia                          | Neuroblast |   |
| Arm (Cyto)     | A/J                               | –          | A*, BL                             | –          | Mild  |
| DE-cad (TM)    | A/J                               | –          | A*, BL                             | –          | Mild  |
| Scrib (Cyto)   | BL                                | –          | C                                  | –          | Mild  |
| Dlg (Cyto)     | BL                                | –          | C                                  | –          | Mild  |
| Cor (Cyto)     | BL                                | –          | C                                  | –          | Mild  |
| Baz (Cyto)     | A                                 | A          | A*                                 | A          | Mild  |
| aPKC (Cyto)    | A                                 | A          | A*                                 | A          | Mild  |
| DmPar-6 (Cyto) | A                                 | A          | A*                                 | A          | Mild  |
| Mir (Cyto)     | C                                 | B          | C                                  | B          | Mild  |
| Crb (TM)       | A                                 | –          | A*                                 | –          | Strong  |
| Dlt (Cyto)     | A                                 | –          | A*                                 | –          | Strong  |

Cyto, cytoplasmic; TM, transmembrane; A, apical; B, basal; BL, basolateral; J, adherens junctional; C, cortical.

\* Punctate and fragmented staining around the cell boundary.

marker Cor at stage 14 (Fig. 3f). Table 1 summarizes the expression patterns of a battery of cellular polarity markers we have examined in *sdt* mutants, showing that all apicolateral and basolateral markers tested are mislocalized in *sdt* mutant epithelia.

Bazooka (Baz), DmPar-6 and atypical protein kinase C (aPKC)<sup>21</sup> form a complex essential for both neuronal and epithelial polarity, and resemble Sdt in their epithelial expression and subcellular localization (Fig. 3a, c, g). As early as stage 7 these proteins all become mislocalized and form random aggregates around the apical cell boundary in epithelial cells (Fig. 3b, d, g, and data not shown). However, their apical localization in delaminating and dividing neuroblasts remains largely normal not only in zygotic *sdt* mutant embryos but also in germline clone embryos in which both maternal and zygotic *sdt* contributions are removed (Fig. 3h and data not shown). Likewise, the basal localization of Miranda (Mir)<sup>22</sup> in neuroblasts was unaffected in *sdt* zygotic or germline clone embryos (Fig. 3i). Similar results were also seen in zygotic *crb* mutants (data not shown), indicating that epithelial but not

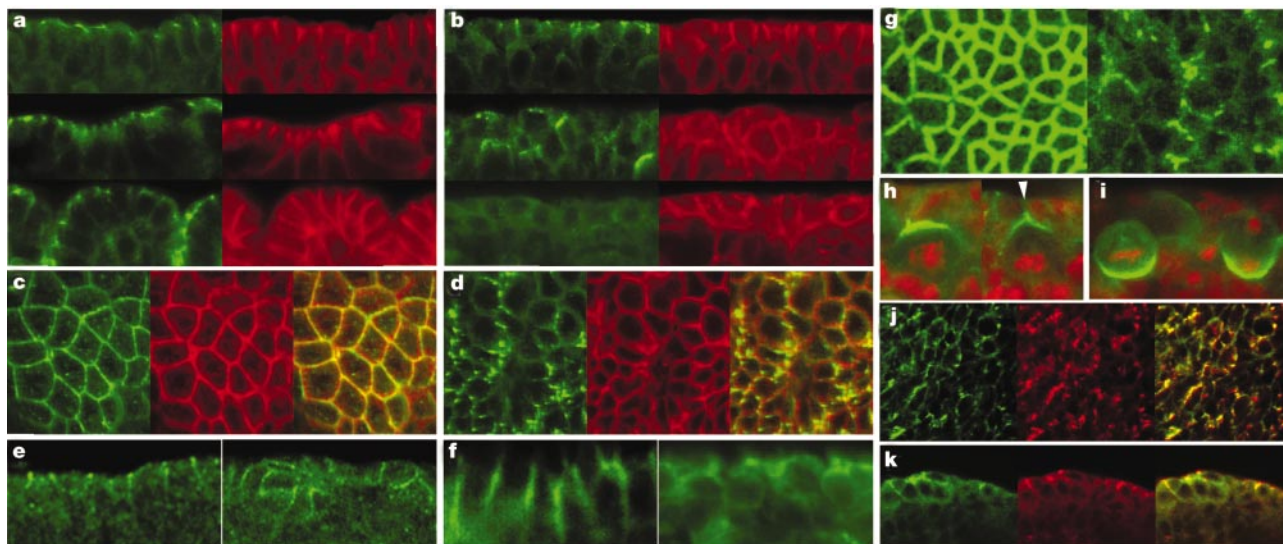


**Figure 3** Characterization of polarity phenotype in *sdt* mutants. **a–d**, Epithelial expression and localization of Baz (green) and Dlg (red) in wild-type (**a, c**) and *XP96* germline clone embryos (**b, d**), shown in cross section at stages 7–8, 11–12 and 14 (**a, b**, from top to bottom), respectively, and in tangential section at stage 9 (**c, d**; right panels are merged images). Note the irregular cell shape and multilayered epithelial structure revealed by Dlg staining in *XP96* mutants at stages 11–12 and 14. **e**, Scrib localization in stage 10–11 wild-type (left) and *XN05* mutant (right) epithelia are very similar to that of Dlg. **f**, Cor is localized to septate junctions in the wild type (left), but appears to be mislocalized into cytoplasm in *XN05* mutant (right). Embryos are at stage 14. **g**, Similar to Baz, aPKC is

uniformly localized to the apical cell cortex of wild-type epithelia (left), but is mislocalized into random aggregates around apical cell boundaries in *XN05* mutant embryos (right). Embryos in **g–k** are all at stage 10. **h, i**, Apical crescent of Baz (**h**) and basal crescent of Mir (**i**) in neuroblasts are both unaffected in *XP96* germline clone embryos that lack both zygotic and maternal *sdt* products. Arrowhead in **h** highlights a Baz ‘stalk’ expanding into the crescent. In **h** and **i**, DNA is stained with PI (red). **j, k**, Although Arm (green) and Baz (red) are mislocalized in *sdt* mutant embryos, they remain largely colocalized around apical cell boundaries (**j**, tangential view, *XP96* germline clone embryo; **k**, cross section view, *XN05* mutant embryo). Right panels are merged images.

neuroblast polarity requires Sdt and Crb.

We wondered how neuroblasts retained their normal apicobasal polarity in *sdt* mutants. Unlike Crb and Dlt (see below), the expression levels of Baz, DmPar-6 and aPKC are not significantly reduced in *sdt* mutants before stage 13 (Fig. 3a–d). Moreover, Baz remains colocalized with Arm/DE-cad in the disrupted AJs (Fig. 3j, k), indicating a residual apicobasal polarity in *sdt* mutants. This is probably due to partial redundancy between Baz and Sdt, as removing zygotic copies of *baz* significantly enhances the null phenotype of *sdt*<sup>16</sup>. This residual polarity retains Baz apically in *sdt* mutants, so that as a neuroblast delaminates Baz is still concentrated in the apical stalk structure<sup>7,8</sup> that expands into an apical crescent (Fig. 3h).

Crumbs, a transmembrane protein with EGF-like repeats, is an apical determinant for establishing apicobasal polarity in embryonic epithelia<sup>6,23,24</sup>. The *sdt* and *crb* mutants exhibit nearly identical defects in epithelial apicobasal polarity, and *crb* and *sdt* function in a common genetic pathway<sup>9,19,20</sup>. We found precise colocalization of Sdt and Crb throughout embryonic development in all cells examined (Fig. 4a–d) except for those in sensory organs: Sdt but not Crb is at the distal dendrites of sensory neurons (Fig. 4e). In epithelial cells Crb and Sdt are mutually dependent for their localization and stability. There is a marked reduction of the protein levels of Crb in *sdt* mutants<sup>9</sup> and of Sdt in *crb* mutants after gastrulation. In both cases, instead of the normal apicolateral distribution, these proteins are found in sparse and discrete random spots (Fig. 4f and g). Dlt, which interacts with the Crb intracellular domain, is distributed similarly to Crb in *sdt* mutants (Fig. 4h), although its early expression and localization during cellularization is not affected even in *sdt* germline clone embryos (data not shown). Conversely, overexpression of the Crb intra-

cellular domain (Crb-intra) is sufficient to cause a ‘dominant’ phenotype, disrupting cell polarity, expanding the apical domain, and displacing endogenous Crb into cytoplasm<sup>23,24</sup>. In such embryos we find that a large fraction of Sdt, together with Crb and Crb-intra, is also displaced away from the membrane into the cytoplasm (Fig. 4i).

To test whether the mutual dependence of Sdt and Crb is due to their physical interaction, we carried out a GST::Crb-intra pull-down assay using *in vitro* translated <sup>35</sup>S-labelled Sdt. Both SdtA and SdtB bind specifically to Crb-intra (Fig. 4k). Two domains of Crb-intra are known<sup>23</sup>, the C-terminal domain containing the EERLI motif, and the amino-terminal domain containing amino acids, such as Y10 and E16, that are conserved in Crb and its *C. elegans* homologues<sup>23</sup> (Fig. 4j). Mutation in either domain abolishes the ability of Crb-intra to rescue the *crb* phenotype, but only the EERLI motif is required for inducing the dominant overexpression phenotype of Crb-intra<sup>23</sup>. In the *in vitro* binding assay, binding of Sdt to Crb-intra was nearly abolished by removal of the C-terminal EERLI motif, but was not affected by Y10A and/or E16A mutations (Fig. 4k), indicating that Crb binds Sdt with its C-terminal EERLI motif.

The same C-terminal EERLI is also required for Dlt to bind to Crb<sup>23</sup>. It will be of interest to determine whether Sdt and Dlt bind Crb cooperatively to form a tertiary complex, or whether they compete with each other for binding to the Crb intracellular domain. We did not detect any direct binding between Dlt and Sdt using the same *in vitro* GST pull-down assay (data not shown). However, MAGUK proteins frequently show intramolecular auto-inhibition between different binding motifs<sup>25,26</sup> so it remains possible that Sdt binds Dlt only after it first binds to Crb.

Thus, whereas the Crb–Sdt (and possibly Dlt) pathway controls

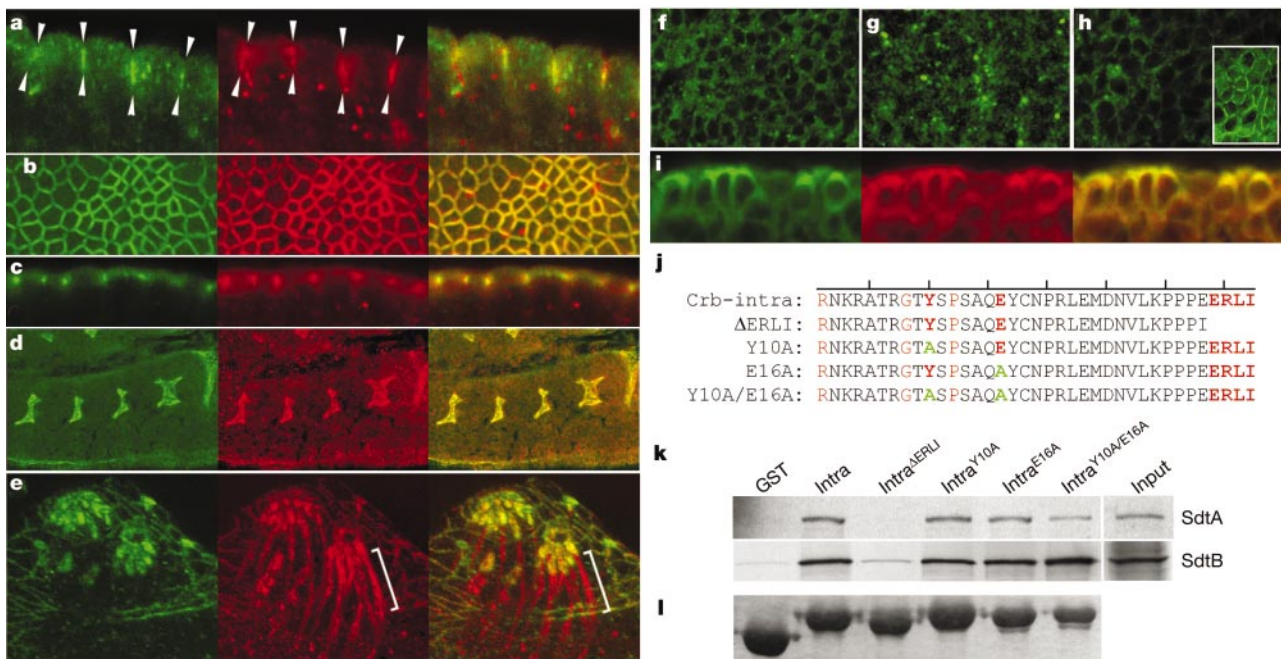


**Figure 4** Sdt interacts with Crb. **a–d**, Colocalization of Crb (green) and Sdt (red) in embryonic epithelial cells. **a**, Cross section, stage 5–6; **b**, tangential view, stage 11; **c**, stage 9, cross section; **d**, stage 11, cross section, tracheal pits. In **a–e** and **i**, right panels are merged images. Vertical pairs of arrowheads in **a** highlight the Sdt and Crb distribution along the apicolateral cortex. **e**, Expression of Crb (green) and Sdt (red) in antennomaxillary complexes in stage 16 embryo. Here, Sdt but not Crb is expressed in the distal dendrites of the sensory neurons (brackets). **f**, Crb localization is severely disrupted and the protein level is reduced in stage 10 *sdt*<sup>XN05</sup> zygotic mutant epithelia. **g**, Sdt localization and expression in epithelia is similarly disrupted and reduced in stage 10 *crb*<sup>1TA22</sup> zygotic mutants. **h**, Epithelial expression of Dlt in *sdt*<sup>XN05</sup> stage 10 mutant embryo

looks similar to Crb expression in **f**. Inset, Dlt expression in the wild type. **i**, Stage 9 embryo overexpressing Crb-intra shows redistribution and colocalization of endogenous Crb (green) and Sdt (red) to the cytoplasm and the expanded apical surface. **j**, Sequences of Crb intracellular domain and different mutants used in GST pull-down experiments (**k**). Conserved amino acids in Crb and its *C. elegans* homologues (not shown) are in red, and mutated amino acids are in green. Residues implicated in Crb function in mutagenesis studies<sup>23</sup> are in bold. **k**, *In vitro* GST pull-down assay demonstrating the interaction between Crb-intra and <sup>35</sup>S-labelled SdtA and SdtB. In the Input panel, only half the amount of the <sup>35</sup>S-labelled SdtA and SdtB proteins were loaded owing to the limitation of loading volume. **l**, SDS-PAGE gel showing the relative amount of protein used in assays in **k**.

the epithelial but not neuroblast polarity, the Baz–DmPar–6–aPKC complex affects both epithelial and neuroblast polarity. Proteins in both pathways are expressed in epithelial cells with identical apico-lateral localization patterns<sup>7,8,12,21</sup> (data not shown) but only Baz–DmPar–6–aPKC are expressed in neuroblasts. In epithelia, these two pathways are probably partially redundant in controlling apicobasal polarity. Their role in regulating ZA formation seems to be the key to their epithelial and cuticle phenotypes. Sdt and Crb colocalize in epithelia and together serve as apical determinants, but only partially overlap and are likely to serve different functions in sensory organs. A mutation in a human Crb homologue has been implicated as the cause of one form of retinitis pigmentosa<sup>27</sup>, suggesting a potential role for the Crb family of proteins in the localization of a sensory transduction complex<sup>28</sup>. The localization of Sdt to the dendritic tip and scolopale cells, the probable sites for sensory transduction, raises the possibility that Sdt may have a role in the development or function of a sensory transduction apparatus. □

## Methods

### Fly stocks and molecular biology

*y w* was used as the wild-type stock in all experiments. For mutant phenotype analysis, *sdt<sup>XN05</sup>* and *sdt<sup>XP96</sup>* were balanced over *FM7,P{fz/lacZ}* and *crb<sup>11A22</sup>* was balanced over *TM3, P{w<sup>+</sup>tmC = 35UZ} Sb<sup>1</sup>. sdt<sup>XP96</sup>* germline clone embryos were produced using the FLP/DFS technique as described<sup>16</sup>. Overexpression of Crb-intra was achieved by crossing upstream activating sequence (UAS)-Crb-intra<sup>23</sup> with the maternal GAL4 driver V32A (provided by D. St Johnston) at 25 °C. Crb-intra fragments were amplified by PCR and inserted into pGEX-4T-1 vector between *EcoRI* and *SalI* to make GST fusion constructs. The GST pull-down assay was carried out as described<sup>22</sup>.

### Allele sequencing

Each *sdt* allele was rebalanced with a green fluorescent protein (GFP) X-chromosome balancer<sup>29</sup>. About 40 GFP-deficient late-stage embryos were picked for DNA preparation. Genomic DNA fragments of *sdt* mutants were amplified with Roche Expand 20kb<sup>PLUS</sup> PCR kit from two embryo equivalents of DNA (pre-denatured before PCR). PCR reactions were set up in duplicate or triplicate and each PCR fragment was independently cloned into pGEM-T Easy+ vector and both strands were fully sequenced.

### Immunofluorescence staining of embryos

Rabbit anti-Sdt serum was affinity purified using Bio-Rad Affi-Gel bound with the same GST:Sdt C-terminal fusion protein used for immunization. Both crude and purified Sdt antiserum failed to detect specific signals in immunoblot experiments. Embryos were fixed with either 4% formaldehyde or 4% paraformaldehyde in 1× PBS buffer. Dilution factors for primary antibodies are given in Supplementary Information. Images were taken on a Bio-Rad MRC600 and a Bio-Rad 1024MP confocal microscope and processed with Adobe Photoshop software.

Received 5 June; accepted 24 September 2001.

- Nüsslein-Volhard, C. & Wieschaus, E. Mutations affecting segment number and polarity in *Drosophila*. *Nature* **287**, 795–801 (1980).
- Jurgens, G., Wieschaus, E., Nüsslein-Volhard, C. & Kluding, H. Mutation affecting the pattern of the larval cuticle in *Drosophila melanogaster*: II. Zygotic loci on the third chromosome. *Roux Arch. Dev. Biol.* **193**, 283–295 (1984).
- Nüsslein-Volhard, C., Wieschaus, E. & Kluding, H. Mutations affecting the pattern of the larval cuticle in *Drosophila melanogaster*: I. Zygotic loci on the second chromosome. *Roux Arch. Dev. Biol.* **193**, 267–282 (1984).
- Wieschaus, E., Nüsslein-Volhard, C. & Jurgens, G. Mutations affecting the pattern of the larval cuticle in *Drosophila melanogaster*: III. Zygotic loci on the X chromosome and fourth chromosome. *Roux Arch. Dev. Biol.* **193**, 296–307 (1984).
- Müller, H.-A. J. Genetic control of epithelial cell polarity: lessons from *Drosophila*. *Dev. Dyn.* **218**, 52–67 (2000).
- Tepass, U., Theres, C. & Knust, E. *crumbs* encodes an EGF-like protein expressed on apical membranes of *Drosophila* epithelial cells and required for organization of epithelia. *Cell* **61**, 787–799 (1990).
- Schober, M., Schaefer, M. & Knoblich, J. A. Bazooka recruits Inscutable to orient asymmetric cell divisions in *Drosophila* neuroblasts. *Nature* **402**, 548–551 (1999).
- Wodarz, A., Ramrath, A., Kuchinke, U. & Knust, E. Bazooka provides an apical cue for Inscutable localization in *Drosophila* neuroblasts. *Nature* **402**, 544–547 (1999).
- Tepass, U. & Knust, E. *crumbs* and *stardust* act in a genetic pathway that controls the organization of epithelia in *Drosophila melanogaster*. *Dev. Biol.* **159**, 311–326 (1993).
- Dimitratos, S. D., Woods, D. F., Stathakis, D. G. & Bryant, P. J. Signalling pathways are focused at specialized regions of the plasma membrane by scaffolding proteins of the MAGUK family. *BioEssays* **21**, 912–921 (1999).
- Gonzalez-Mariscal, L., Betanzos, A. & Avila-Flores, A. MAGUK proteins: structure and role in the tight junction. *Cell Dev. Biol.* **11**, 315–324 (2000).
- Petronczki, M. & Knoblich, J. A. DmPAR-6 directs epithelial polarity and asymmetric cell division of neuroblasts in *Drosophila*. *Nature Cell Biol.* **3**, 43–49 (2001).
- Bhat, M. *et al.* Discs Lost, a novel multi-PDZ domain protein establishes and maintains epithelial polarity. *Cell* **96**, 833–845 (1999).

- Bilder, D. & Perrimon, N. Localization of apical epithelial determinants by the basolateral PDZ protein Scribble. *Nature* **403**, 676–680 (2000).
- Kamberov, E. *et al.* Molecular cloning and characterization of Pals, proteins associated with mLin-7. *J. Biol. Chem.* **275**, 11425–11431 (2000).
- Müller, H.-A. J. & Wieschaus, E. *armadillo*, *bazooka*, and *stardust* are critical for early stages in formation of the zonula adherens and maintenance of the polarized blastoderm epithelium in *Drosophila*. *J. Cell Biol.* **134**, 149–163 (1996).
- Tepass, U. Epithelial differentiation in *Drosophila*. *BioEssays* **19**, 673–682 (1997).
- Tepass, U. & Hartenstein, V. The development of cellular junctions in the *Drosophila* embryo. *Dev. Biol.* **161**, 563–596 (1994).
- Tepass, U. Crumbs, a component of the apical membrane, is required for zonula adherens formation in primary epithelia of *Drosophila*. *Dev. Biol.* **177**, 217–225 (1996).
- Grawe, F., Wodarz, A., Lee, B., Knust, E. & Skaer, H. The *Drosophila* genes *crumbs* and *stardust* are involved in the biogenesis of adherens junctions. *Development* **122**, 951–959 (1996).
- Wodarz, A., Ramrath, A., Grimm, A. & Knust, E. *Drosophila* atypical protein kinase C associates with Bazooka and controls polarity of epithelia and neuroblasts. *J. Cell Biol.* **150**, 1361–1374 (2000).
- Shen, C.-P., Jan, L. Y. & Jan, Y. N. Miranda is required for the asymmetric localization of Prospero during mitosis in *Drosophila*. *Cell* **90**, 449–458 (1997).
- Klebes, A. & Knust, E. A conserved motif in Crumbs is required for E-cadherin localisation and zonula adherens formation in *Drosophila*. *Curr. Biol.* **10**, 76–85 (2000).
- Wodarz, A., Hinz, U., Engelbert, M. & Knust, E. Expression of Crumbs confers apical character on plasma membrane domains of ectodermal epithelia of *Drosophila*. *Cell* **82**, 67–76 (1995).
- Brennan, J. E. *et al.* Localization of postsynaptic density-93 to dendritic microtubules and interaction with microtubule-associated protein 1A. *J. Neurosci.* **18**, 8805–8813 (1998).
- Shin, H., Hsueh, Y.-P., Yang, F.-C., Kim, E. & Sheng, M. An intramolecular interaction between Src homology 3 domain and guanylate kinase-like domain required for channel clustering by Postsynaptic Density-95/SAP90. *J. Neurosci.* **20**, 3580–3587 (2000).
- Den Hollander, A. I. *et al.* Mutations in a human homologue of *Drosophila crumbs* cause retinitis pigmentosa (RP12). *Nature Genet.* **23**, 217–221 (1999).
- Rashbass, P. & Skaer, H. Cell polarity: nailing Crumbs to the scaffold. *Curr. Biol.* **10**, R234–R236 (2000).
- Casso, D., Ramirez-Weber, F. & Kornberg, T. B. GFP-tagged balancer chromosomes for *Drosophila melanogaster*. *Mech. Dev.* **91**, 451–454 (2000).

Supplementary Information accompanies the paper on Nature's website (<http://www.nature.com>).

### Acknowledgements

We are grateful to D. Bilder, M. Bhat, T. Uemura, P. J. Bryant, U. Tepass, E. Knust, E. Wieschaus, Developmental Studies Hybridoma Bank and Bloomington Stock Center for providing fly stocks, antibodies and constructs. We thank S. Barbel, L. Ackerman and S. Younger-Shepherd for technical assistance and M. Rothenberg, D. Cox, S. Abdelilah and U. Tepass for critical comments on the manuscript. B.S. is supported by a grant from the National Institutes of Health. Y.H. is a Research Associate and N.P., L.Y.J. and Y.N.J. are Investigators of the Howard Hughes Medical Institute.

Correspondence and requests for materials should be addressed to Y.N.J. (e-mail: ynjan@itsa.ucsf.edu).

## Drosophila Stardust is a partner of Crumbs in the control of epithelial cell polarity

André Bachmann, Martina Schneider\*, Eva Theilenberg, Ferdi Grawe & Elisabeth Knust

Institut für Genetik, Heinrich-Heine-Universität Düsseldorf, Universitätsstraße 1, 40225 Düsseldorf, Germany

The polarized architecture of epithelial cells depends on the highly stereotypic distribution of cellular junctions and other membrane-associated protein complexes. In epithelial cells of the *Drosophila* embryo, three distinct domains subdivide the lateral plasma membrane. The most apical one comprises the subapical complex (SAC). It is followed by the zonula adherens (ZA) and, further basally, by the septate junction<sup>1</sup>. A core component of the SAC is the transmembrane protein Crumbs, the cytoplasmic domain of which recruits the PDZ-protein Discs Lost into the complex<sup>2,3</sup>. Cells lacking *crumbs* or the functionally related gene *stardust* fail to organize a continuous ZA and to maintain cell

\* Present address: Lund University, Department of Cell & Molecular Biology, S-22184 Lund, Sweden.